
Zeroth-Order Actor-Critic

Yuheng Lei¹, Jianyu Chen^{2 3}, Shengbo Eben Li¹, Sifa Zheng¹

¹School of Vehicle and Mobility, Tsinghua University

²Institute for Interdisciplinary Information Sciences, Tsinghua University

³Shanghai Qizhi Institute

leiyh20@mails.tsinghua.edu.cn, {jianyuchen, lishbo, zsf}@tsinghua.edu.cn

Abstract

The recent advanced evolution-based zeroth-order optimization methods and the policy gradient-based first-order methods are two promising alternatives to solve reinforcement learning (RL) problems with complementary advantages. The former methods work with arbitrary policies, drive state-dependent and temporally-extended exploration, possess robustness-seeking property, but suffer from high sample complexity, while the latter methods are more sample efficient but are restricted to differentiable policies and the learned policies are less robust. To address these issues, we propose a novel Zeroth-Order Actor-Critic algorithm (ZOAC), which unifies these two methods into an on-policy actor-critic architecture to preserve the advantages from both. ZOAC conducts rollouts collection with timestep-wise perturbation in parameter space, first-order policy evaluation (PEV) and zeroth-order policy improvement (PIM) alternately in each iteration. We extensively evaluate our proposed method on a wide range of challenging continuous control benchmarks using different types of policies, where ZOAC outperforms zeroth-order and first-order baseline algorithms.

1 Introduction

Reinforcement learning (RL) has achieved great success in a wide range of challenging domains, including video games [24], robotic control [36], autonomous driving [14], etc. The majority of RL methods formulate the environment as a Markov decision process (MDP) and leverage the temporal structure to design learning algorithms such as Q-learning and policy gradient [44]. Actor-critic methods are among the most popular RL algorithms, which usually introduce two function approximators, one for value function estimation (critic) and another for optimal policy approximation (actor), and optimize these two approximators by alternating between policy evaluation (PEV) and policy improvement (PIM). On-policy actor-critic methods, e.g., A3C [25] and PPO [36], often use critics to construct advantage functions and substitute them for the Monte Carlo return used in vanilla policy gradient [48], which significantly reduces the variance of gradient estimation and improve learning speed and stability. Among existing actor-critic algorithms, a common choice is to use deep neural networks as the function approximators and conduct both PEV and PIM using first-order optimization techniques.

An alternative approach for RL, though less popular, is to ignore the underlying MDP structures and regard RL problems as black-box optimization, and to directly search for the optimal policy in a zeroth-order way, i.e., without using the first-order gradient information. Recent researches have shown that zeroth-order optimization (ZOO) methods, e.g., ES [34], ARS [23, 13] and GA [43, 33], are competitive on common RL benchmarks, even when applied to deep neural network with millions of parameters or with complex heterogeneous architectures like world models [11]. ZOO has several advantages compared to first-order MDP-based RL methods [37, 43, 17, 16, 31]: (1) ZOO is not restricted to differentiable policies [13, 33]; (2) ZOO perturbs the policy in parameter space rather

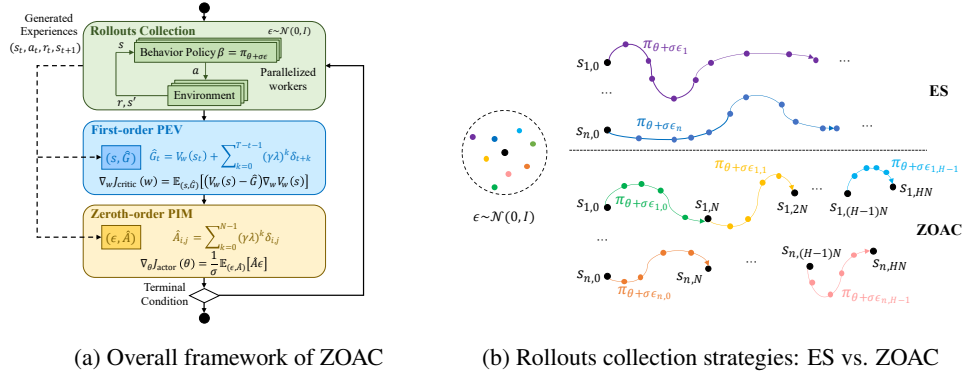


Figure 2: (a) The overall framework of our proposed algorithm ZOAC; (b) Comparison of rollouts collection strategies (with n parallelized samplers): On the top is ES, which performs episode-wise perturbation; on the bottom is ZOAC, which performs N timesteps-wise perturbation.

than in action space, which leads to state-dependent and temporally-extended exploration [34, 16]; (3) Zeroth-order population-based optimization possesses robustness-seeking property and diverse policy behaviors [17].

Despite these attractive advantages, the main limitation of ZOO is its high sample complexity and high variance of the parameter update process, especially in high-dimensional problems. Recent researches have proposed various techniques to improve ZOO, e.g., using orthogonal or antithetic sampling methods [37, 34, 6, 23], identifying a low-dimensional search subspace [22, 7, 38], or subtracting a baseline for variance reduction [37, 10]. One of the major reasons for the sample inefficiency of ZOO is its ignorance of the MDP temporal structures. Many recent researches have tried to combine ZOO and first-order MDP-based RL into hybrid methods, e.g., run evolutionary algorithms in parallel with off-policy RL algorithms and optimize the population of policies with information from both sides [16, 29, 4], or inject parameter noise into existing RL algorithms for efficient exploration [28, 9]. However, existing hybrid methods still conduct first-order gradient-based policy improvement (at least as a part), which reimposes a differentiable requirement on the policy. A more detailed discussion of the related works is attached in Appendix A.

In this paper, we propose a novel Zeroth-Order Actor-Critic algorithm (ZOAC), which makes several **contributions** more beneficial than prior arts. **Firstly**, ZOAC unifies first-order and zeroth-order RL methods into an actor-critic architecture by conducting first-order policy evaluation (PEV) to update the critic and zeroth-order policy improvement (PIM) to update the actor. In such a way, complementary advantages of both methods are preserved, such as wide versatility to policy parameterization, robustness seeking property, state-dependent and temporally-extended exploration. **Secondly**, we modify the rollouts collection strategy from an episode-wise perturbation as in traditional zeroth-order methods to a timestep-wise perturbation for better exploration, and derive the zeroth-order policy gradient under this setting. We point out that a critic network can be introduced to estimate the state-value function and trade-off between bias and variance. We then propose a practical algorithm that utilizes several parallelized rollout workers and alternates between first-order PEV and zeroth-order PIM based on generated experiences in each iteration. **Thirdly**, we extensively evaluate ZOAC on a wide range of challenging continuous control benchmarks from OpenAI gym [5], using different types of policies, including linear policies and neural networks with full or compact architectures. Experiment results show that ZOAC outperforms zeroth-order and first-order baseline algorithms in sample efficiency, final performance, and the robustness of the learned policies. Furthermore, we conduct ablation studies to demonstrate the indispensable contribution of the modified rollouts collection strategy and the introduced critic network to ZOAC.

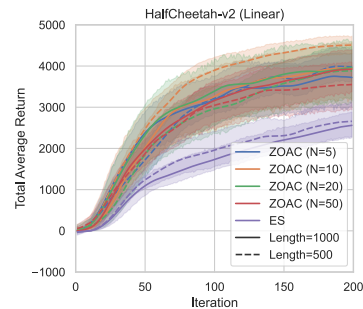
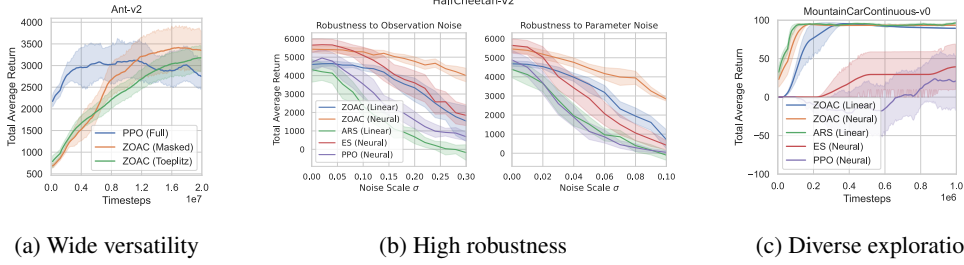


Figure 1: Performance comparison between ES and ZOAC gradient estimates (Section 3.2)



(a) Wide versatility (b) High robustness (c) Diverse exploration

Figure 3: Some benefits of ZOAC inherited from evolutionary methods: (a) *Wide versatility*: ZOAC successfully learned compact/non-differentiable policies achieving better performance with much fewer parameters (less than 10 percent) in high dimensional environments; (b) *High robustness*: Population-based optimization scheme and consistent perturbation implies better robustness and generalization of the learned policies; (c) *Diverse exploration*: ZOAC drives diversified and temporally-extended exploration in sparse reward environments and does not easily get stuck in local optima.

2 Preliminary and Notation

2.1 From Policy Gradient to Actor-Critic

In standard MDP-based RL settings, the environment is usually formulated as an MDP defined as $(\mathcal{S}, \mathcal{A}, \mathcal{P}, r)$, where \mathcal{S} is the state space, \mathcal{A} is the action space, $\mathcal{P} : \mathcal{S} \times \mathcal{A} \times \mathcal{S} \rightarrow \mathbb{R}$ is the transition probability matrix, $r : \mathcal{S} \times \mathcal{A} \rightarrow \mathbb{R}$ is the reward function. The return is defined as the total discounted future reward $G_t = \sum_{i=0}^{\infty} \gamma^i r(s_{t+i}, a_{t+i})$, where $\gamma \in (0, 1)$ is the discount factor. The behavior of the agent is controlled by a policy $\pi(a|s) : \mathcal{S} \times \mathcal{A} \rightarrow [0, 1]$, which maps states to a probability distribution over actions. The value function is defined as the expected return under policy π : $V^\pi(s) = \mathbb{E}_\pi[G_t | s_t = s]$ and $Q^\pi(s, a) = \mathbb{E}_\pi[G_t | s_t = s, a_t = a]$. The goal of MDP-based RL is to find an optimal policy that maximizes the expectation of state-value function under a certain state distribution. Denoting a policy parameterized with θ as π_θ , the objective function can be written as:

$$J_{\text{PG}}(\theta) = \mathbb{E}_{s \sim d_0} [V^{\pi_\theta}(s)] \quad (1)$$

where d_0 is the initial state distribution. The policy gradient theorem [44] holds for any differentiable policy π_θ . The vanilla policy gradient REINFORCE given by Williams [48] is as follows:

$$\nabla_\theta J_{\text{PG}}(\theta) = \mathbb{E}_{s_t \sim d_{\pi_\theta}, a_t \sim \pi_\theta} [G_t \nabla_\theta \log \pi_\theta(a_t | s_t)] \quad (2)$$

The discounted state distribution is denoted as $d_{\pi_\theta}(s') := \int_{\mathcal{S}} \sum_{t=0}^{\infty} \gamma^t d_0(s) p(s \rightarrow s', t, \pi_\theta) ds$. Vanilla policy gradient suffers from high variance since it directly uses Monte Carlo return from sampled trajectories. Actor-critic methods improved upon it, which usually introduce a critic network to estimate the value function and serve as a baseline to substitute the expected return G_t with a proper form of advantage function A_t , for example, TD residual [25], or generalized advantage estimation (GAE) [35]. However, the above policy gradient based methods can only be applied to differentiable policies, and may be unavailable when a non-differentiable controller needs to be optimized.

2.2 Evolution Strategies (ES)

Existing ZOO methods focus on episodic RL problems with finite horizon and treat them as black-box optimization. In these cases, the length of trajectories is limited and the discount factor γ is usually set as 1. Evolution strategies (ES) is one of the most popular algorithms of ZOO, which optimizes a Gaussian smoothed objective function:

$$J_{\text{ES}}(\theta) = \mathbb{E}_{\epsilon \sim \mathcal{N}(0, I)} \mathbb{E}_{s \sim d_0} [V^{\pi_{\theta+\sigma\epsilon}}(s)] \quad (3)$$

where d_0 is the initial state distribution and σ is the standard deviation of the Gaussian noise added to the policy. The ES gradient can be derived using the log-likelihood ratio trick and the probability density function of Gaussian distribution [27, 34]:

$$\nabla_\theta J_{\text{ES}}(\theta) = \frac{1}{\sigma} \mathbb{E}_{\epsilon \sim \mathcal{N}(0, I)} \mathbb{E}_{s \sim d_0} [V^{\pi_{\theta+\sigma\epsilon}}(s) \epsilon] \quad (4)$$

In practice, the expectation over Gaussian distribution can be approximated by sampling n noise samples $\{\epsilon_i\}_{i=1,\dots,n}$, and the corresponding state value $V^{\pi_{\theta+\sigma\epsilon_i}}$ can be approximated by the episodic return $G_i = \sum_{t=0}^T \gamma^t r(s_t, a_t)$ of the sample trajectory of length T collected with policy $\pi_{\theta+\sigma\epsilon_i}$:

$$\nabla_{\theta} J_{\text{ES}}(\theta) \approx \frac{1}{n\sigma} \sum_{i=1}^n G_i \epsilon_i \quad (5)$$

The gradient estimator in Equation (5) only relies on the episodic returns of each evaluated random directions, so it is applicable to non-differentiable policies. Besides, each perturbed policy remains deterministic in one trajectory, which leads to temporally-extended exploration. Furthermore, the Gaussian smoothed objective also improves robustness of the learned policies in parameter space.

3 Zeroth-Order Actor-Critic

3.1 From ES to ZOAC

In this section, we will derive an improved zeroth-order gradient combining the actor-critic architecture for policy improvement. We start from improving the sample efficiency and stability of ES. Most of the existing ES methods applied to RL optimize a deterministic policy [34, 23], where the exploration is driven by parameter perturbation. Without loss of generality, we follow them in the following derivations and algorithm design. A deterministic policy parameterized with θ is denoted as $\pi_{\theta} : \mathcal{S} \rightarrow \mathcal{A}$, which directly maps states to actions.

In ES, the policy is perturbed in parameter space at the beginning of an episode and remains unchanged throughout the trajectories. If a large number of random directions n is evaluated, the sample complexity will increase significantly. However, since the zeroth-order gradient is estimated as the weighted sum of several random directions, it exhibit excessively high variance when n is small [3], which may greatly harm the performance. Therefore, it is essential to trade-off this contradictory between sample efficiency and variance.

To encourage sufficient exploration and low variance while maintaining high sample efficiency, here we consider perturbing the policy at every timestep, i.e., the Gaussian noise ϵ is sampled identically and independently at every timesteps. We regard it as a stochastic exploration policy $\beta = \pi_{\theta+\sigma\epsilon}$, where σ is the standard deviation and $\epsilon \sim \mathcal{N}(0, I)$ is Gaussian parameter noise. Our objective is to maximize the expected return obtained by the exploration policy β :

$$J_{\text{ZOAC}}(\theta) = \mathbb{E}_{s \sim d_0} [V^{\beta}(s)] \quad (6)$$

The zeroth-order policy gradient under this setting can be derived as follows. The proof adopts a similar scheme to [45] and [40] and is provided in Appendix B.

Theorem 1. *For MDP that satisfies regularity conditions in Appendix B, zeroth-order policy gradient of Equation (6) can be presented as:*

$$\nabla_{\theta} J_{\text{ZOAC}}(\theta) = \frac{1}{\sigma} \mathbb{E}_{s_t \sim d_{\beta}} \mathbb{E}_{\epsilon \sim \mathcal{N}(0, I)} [Q^{\beta}(s_t, \pi_{\theta+\sigma\epsilon}(s_t)) \epsilon] \quad (7)$$

Similar to on-policy policy gradient methods, we can approximate this gradient via on-policy samples and derive different variants of this zeroth-order policy gradient. We first rewrite it into the form of TD residual:

$$\nabla_{\theta} J_{\text{ZOAC}}(\theta) = \frac{1}{\sigma} \mathbb{E}_{s_t \sim d_{\beta}} \mathbb{E}_{\epsilon \sim \mathcal{N}(0, I)} \mathbb{E}_{s_{t+1} \sim \mathcal{P}} [(r(s_t, \pi_{\theta+\sigma\epsilon}(s_t)) + \gamma V^{\beta}(s_{t+1}) - V^{\beta}(s_t)) \epsilon] \quad (8)$$

Note that in Eq. (8), $V^{\beta}(s_t)$ can be subtracted as a baseline for variance reduction because: (1) V^{β} itself is already an expectation over ϵ and is no longer correlated to the noise ϵ ; (2) the zero mean property of the Gaussian noise ϵ .

Compared to ES which uses unbiased but high variance Monte Carlo return to evaluate each perturbed policy, the performance of each random direction here is estimated by one-step TD residual with

low variance. In practice, a common approach is to introduce a critic network $V_w(s)$ to estimate the state-value function V^β , which may lead to high bias in this form of advantage estimation.

To trade-off between bias and variance, we consider extending our derivation further to the case where the behavior policy β runs forward N timesteps with each sampled random noise instead of one timestep only, as shown in Figure 2b. Eq. (8) can be extended to the N -step TD residual variant:

$$\nabla_\theta J_{\text{ZOAC}}(\theta) = \frac{1}{\sigma} \mathbb{E}_{s_t \sim d^\beta} \mathbb{E}_{\epsilon \sim \mathcal{N}(0, I)} \mathbb{E}_{\mathcal{P}} \left[\left(\sum_{i=0}^{N-1} \gamma^i r_i + \gamma^N V^\beta(s_{t+N}) - V^\beta(s_t) \right) \epsilon \right] \quad (9)$$

where r_i refers to $r(s_{t+i}, \pi_{\theta+\sigma\epsilon}(s_{t+i}))$ and $\mathbb{E}_{\mathcal{P}}$ means expectation over N -step transition dynamics. Similar to one-step case, the cumulative reward within N step can be estimated from sampled experiences when s_t is the first state of the trajectory fragment collected with a certain perturbed policy $\pi_{\theta+\sigma\epsilon}$. By introducing a critic network and choosing an appropriate length N , this N -step residual advantage function contributes to achieving a good trade-off between the bias and variance.

3.2 Comparison of Gradient Estimators.

Theoretical analysis on variance. We analyze the variance of these two types of gradient estimators, ZOAC gradient and ES gradient. The budget of timestep of one trajectory $N \times H$ is identical for both algorithms: in ZOAC, each perturbed policy run forward N steps, and H is the number of sampled random directions in one trajectory; in ES, only one perturbed policy is sampled and run forward $N \times H$ steps. If we denote the accumulative reward obtained within $N \times H$ timesteps in ES as $\hat{V}_{NH}^{\pi_{\theta+\sigma\epsilon}}$ and the N -step TD residual in ZOAC as $\hat{A}_N^{\pi_{\theta+\sigma\epsilon}}$. We can then estimate the zeroth-order policy gradient according to Eq. (4) and (9) respectively:

$$\nabla_\theta \hat{J}_{\text{ES}}(\theta) = \frac{1}{n\sigma} \sum_{i=1}^n \hat{V}_{NH}^{\pi_{\theta+\sigma\epsilon_i}} \epsilon_i \quad (10)$$

$$\nabla_\theta \hat{J}_{\text{ZOAC}}(\theta) = \frac{1}{nH\sigma} \sum_{i=1}^{nH} \hat{A}_N^{\pi_{\theta+\sigma\epsilon_i}} \epsilon_i \quad (11)$$

We now give the upper bound of variance for these two gradient estimators. Following the variance analysis scheme in [49], variance is defined as the trace of the covariance matrix of gradient vectors $\text{Var}(\mathbf{g}) = \sum_{l=1}^d \mathbb{E}[(g_l - \mathbb{E}[g_l])^2]$, where $\mathbf{g} = (g_1, g_2, \dots, g_d)^\top$. We can derive the variance bound as follows with the proof provided in Appendix B.

Theorem 2. *If the reward $|r(s, a)| < \alpha$, the critic network output $|V_w(s)| < \varphi$, and n trajectories with length of $N \times H$ timesteps are collected in one iteration, the upper bounds of the variance for gradient estimators in Eq. (10) and (11) are:*

$$\text{Var}[\nabla_\theta \hat{J}_{\text{ES}}(\theta)] \leq \frac{(1 - \gamma^{NH})^2 \alpha^2 d}{n\sigma^2(1 - \gamma)^2} \quad (12)$$

$$\text{Var}[\nabla_\theta \hat{J}_{\text{ZOAC}}(\theta)] \leq \frac{((1 - \gamma^N)\alpha + (1 - \gamma)(1 + \gamma^N)\varphi)^2 d}{nH\sigma^2(1 - \gamma)^2} \quad (13)$$

We can compare their variance in a more intuitive way: if $N \times H = 1000$, $\gamma = 0.99$, and assume that $\varphi \approx \frac{\alpha}{1-\gamma}$, the difference of variance bounds becomes $\overline{\text{Var}}[\nabla_\theta \hat{J}_{\text{ZOAC}}(\theta)] - \overline{\text{Var}}[\nabla_\theta \hat{J}_{\text{ES}}(\theta)] \approx (\frac{4}{H} - 1) \frac{10000\alpha^2 d}{n\sigma^2}$, which decreases with H and drops below zero when $4 < H \leq 1000$ (i.e., N is smaller than 250). This suggests that although same amount of data is collected, an appropriate rollout length N can indeed reduce variance of the gradient estimators. Besides, both variance bound are inversely proportional to n , which urges us to collect more trajectories.

Empirical analysis via performance comparison. Choosing appropriate rollout length N of each perturbed policies may achieve a good trade-off between bias and variance. We perform an ablation study as in Figure 1 to understand the influence of N . We compare these two gradient estimators on HalfCheetah-v2, the former conducting timesteps-wise perturbation and the latter conducting episode-wise perturbation. We use linear policies in both methods and set hyperparameters to the same (directly taken from [23]), including the standard deviation of parameter noise σ , the learning rate of policy α_{actor} , and also the budget of trajectories within one iteration. Results show that rollout lengths N in a large range leads to significant improvement on sample efficiency compared to ES.

Algorithm 1 Zeroth-Order Actor-Critic (ZOAC)

```
1: Initialize: policy parameters  $\theta$ , critic network parameters  $w$ 
2: for each iteration do
3:   for each worker  $i = 1, 2, \dots, n$  do
4:     for  $j = 0, 1, \dots, H - 1$  do
5:       Sample  $\epsilon_{i,j} \sim \mathcal{N}(0, I)$ 
6:       Run perturbed policy  $\pi_{\theta+\sigma\epsilon_{i,j}}$  in environment for  $N$  timesteps
7:       Compute advantage function  $\hat{A}^{\pi_{\theta+\sigma\epsilon_{i,j}}}$  according to Equation (16)
8:     end for
9:     Compute the state-value target  $\hat{G}_t$  for each state  $s_t$  according to Equation (14)
10:  end for
11:  Collect  $(s, \hat{G})$  for critic update and  $(\epsilon, \hat{A})$  for actor update
12:  Update  $w$  with batch size  $L$  through SGD by minimizing Equation (15) for  $M$  epoches
13:  Update  $\theta$  along the zeroth-order gradient direction estimated in Equation (17)
14: end for
```

3.3 Practical Algorithm

We propose the Zeroth-Order Actor-Critic (ZOAC) algorithm, which unifies first-order and zeroth-order methods into an on-policy actor-critic architecture by conducting rollouts collection with timestep-wise perturbation in parameter space, first-order policy evaluation (PEV) and zeroth-order policy improvement (PIM) alternately in each iteration. The overall framework of ZOAC is shown in Figure 2 and the pseudocode is summarized in Algorithm 1. In each iteration, parallelized workers will collect rollouts in the environment with perturbed policies, then the agent trains the critic network to estimate state-value function under the exploration policy, and finally improves the policy along the zeroth-order gradient direction.

Rollouts collection. The rollouts collection strategy is illustrated briefly in Figure 2b, which is a parallelized version with n workers. If we denote the t -th state sampled by the i -th worker as $s_{i,t}$, the rollout strategy can be described as: when reaching states in $\{s_{i,jN}\}$, where $j \in \mathbb{N}$, a new random direction $\epsilon_{i,j}$ is sampled and the behavior policy is perturbed; when reaching other states, the deterministic behavior policy remains unchanged. It’s worth noting that the notation is only for the continuing case where an episode is never done. In episodic tasks, the rollout length $1 \leq N_{i,j} \leq N$ actually varies between different perturbed policies $\pi_{\theta+\sigma\epsilon_{i,j}}$ since an episode may terminate at any time. However, we still use N to denote the rollout length of each perturbed policy for brevity.

A limit case of our proposed strategy is that when N is chosen as the episode length and the critic network is turned off (i.e., $V_w(s) \equiv 0$), the algorithm actually degenerates into ES, since all perturbed policies are evaluated by running a whole episode, and the episodic return is used as the fitness score.

First-order PEV. The state-value function of the behavior policy $V^\beta(s)$ can be estimated by a jointly optimized critic network $V_w(s)$, which aims to minimize the MSE loss between the network output and state-value target. In each iteration, in total $n \times N \times H$ states and the corresponding target values (s, \hat{G}) are calculated and used for critic training. In a trajectory with length T , the target value \hat{G}_t for each state s_t is calculated as [1]:

$$\hat{G}_t = V_w(s_t) + \sum_{k=0}^{T-t-1} (\gamma\lambda)^k [r_{t+k} + \gamma V_w(s_{t+k+1}) - V_w(s_{t+k})] \quad (14)$$

where $0 < \lambda < 1$ is a hyperparameter to control the trade-off between bias and variance of the value target. In Figure 2, the one-step TD residual of each state is denoted as δ for simplicity. The objective function of PEV can be written as:

$$J_{\text{critic}}(w) = \mathbb{E}_{(s, \hat{G})} \left[\frac{1}{2} (V_w(s) - \hat{G})^2 \right] \quad (15)$$

In practice, the critic network is constructed as a neural network and updated through several epochs of stochastic gradient descent in each iteration.

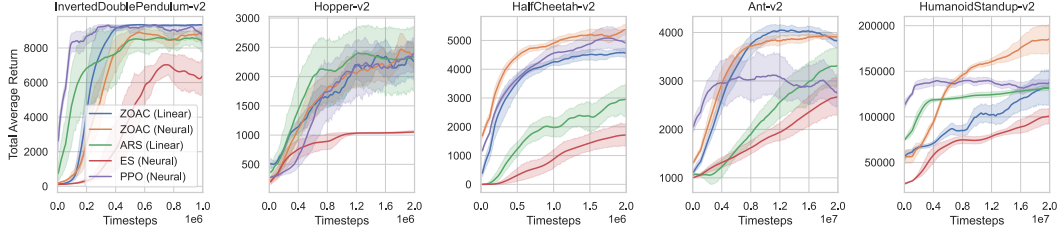


Figure 4: Learning curves on MuJoCo benchmarks. Exploration noise are turned off for evaluation. The solid lines correspond to the mean and the shaded regions to the 95% confidence interval over 10 trials using a fixed set of random seeds. All curves are smoothed uniformly for visual clarity.

Zeroth-order PIM. We calculate the zeroth-order gradient with $n \times H$ random directions and the corresponding advantage function as (ϵ, \hat{A}) . Similar to state value estimation, we perform the generalized advantage estimation (GAE) trick [35] to further control the bias-variance trade-off, as well as the advantage normalization trick. Following the notations in Figure 3, the advantage function can be written as:

$$\hat{A}_N^{\pi_{\theta} + \sigma \epsilon_{i,j}} = \sum_{k=0}^{N-1} (\gamma \lambda)^k [r_{i,jN+k} + \gamma V_w(s_{i,jN+k+1}) - V_w(s_{i,jN+k})] \quad (16)$$

where λ is the same as in Equation (14). The zeroth-order gradient can be then estimated as the weighted sum of the sampled random directions:

$$\nabla_{\theta} J_{\text{actor}}(\theta) \approx \frac{1}{nH\sigma} \sum_{i=1}^n \sum_{j=0}^{H-1} \hat{A}_N^{\pi_{\theta} + \sigma \epsilon_{i,j}} \epsilon_{i,j} \quad (17)$$

4 Experiments

4.1 Overall Performance Evaluation

We evaluate the performance of ZOAC on the MuJoCo continuous control benchmarks [47] in OpenAI Gym [5]. We choose Evolution Strategies (ES) [34, 19] and Augmented Random Search (ARS) [23] as evolution-based zeroth-order baselines and proximal policy optimization (PPO) [36, 32] as a first-order on-policy actor-critic baseline. We aim to examine the advantage of ZOAC over each of its counterparts in the experiments. Some additional results and analysis are attached in Appendix E.

We use two different types of policies: linear policies for ARS and ZOAC (linear), neural networks with (64, 64) hidden nodes and tanh nonlinearities for ES, PPO and ZOAC (neural). For a fair comparison, we enable observation normalization for all methods, which has been proved effective no matter in first-order methods or zeroth-order methods [23, 1]. When using neural networks as actors, we also use layer normalization [2] in ZOAC and virtual batch normalization in ES [34]. Both of them ensure the diversity of behaviors among the population, while the former is less computationally expensive. We summarize the implementation details of ZOAC in Appendix C and follow the recommended hyperparameter settings listed in the related papers or code repositories.

Sample Efficiency. Figure 4 presents the learning curves on five continuous control tasks. ZOAC matches or outperforms baseline algorithms across tasks in learning speed, final performance, and variance over trials. One thing worth mentioning is that both the zeroth-order baseline methods perform reward shaping to resolve the local optima problem: ARS subtracts the survival bonus from rewards (1 in Hopper and Ant), while ES transforms the episodic returns into rankings. Although these tricks improve the performance, they also alter the update directions of the policies and make it difficult to determine what is the real objective function being optimized. ZOAC, however, surpasses ES and ARS without relying on specific heuristic tricks, which can be attributed to the introduction of critic network and the construction of advantage estimations in policy improvement.

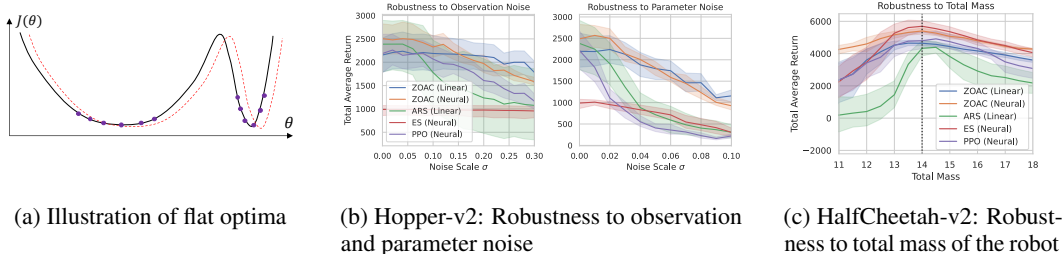


Figure 5: Robustness and generalization comparison of the learned policies.

Robustness and generalization. The objective function of ZOAC aims to maximize the expected state-value of the stochastic behavior policy that contains parameter noise all the time, which intuitively encourages the agent to find a wider optima and leads to better generalization and robustness [15, 12], as illustrated in Figure 5a. Hence, we evaluate the learned policies after convergence under two types of noise, observation noise and parameter noise. Extra observation noise is added to the normalized observation at each timestep, which leads to a slightly different objective function surface. Extra parameter noise is added at the beginning of each trajectories, which pushes the learned policy to its neighborhood. The results in HalfCheetah-v2 (policies at $2e7$ timesteps for ES and ARS, $2e6$ for else) and Hopper-v2 (policies at $2e6$ timesteps for all) are presented in Figure 3b and 5b, respectively. We also directly examine generalization in Figure 5c by modifying the robot parameters. Results show that in general the policies learned by ZOAC, no matter linear ones or neural ones, possess higher robustness and suffer much milder performance degradation rate under both observation noise and parameter noise, which can be ascribed to the robustness-seeking property of our method.

Exploration in sparse reward environment.

We apply all methods on MountainCarContinuous-v0, in which the car is rewarded +100 only when it achieves the goal and penalized by the action output at every timestep. Policy gradient methods usually struggle on this problem because the reward is sparse and delayed, while zeroth-order methods can better handle reward sparsity by nature. We plot the learning curves in Figure 3c, showing that ZOAC can learn a good solution consistently while PPO and ES get stuck occasionally. We also visualize the learned policies in Figure 6. The neural policy learned by ZOAC obtains the second highest average return within the shortest episode length. As for linear policies, the one learned by ZOAC also tends to achieve the goal in a shorter episode length than the one learned by ARS. We attribute this to the usage of discounting factor, which pushes the agent to perform higher actions and achieve the goal as early as possible. ZOAC outperforms PPO both in final performance and training stability over different random seeds, due to its more efficient and diversified exploration, which facilitates escaping local optima and is essential to solve this task.

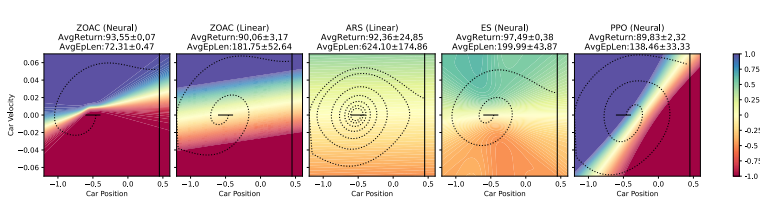


Figure 6: Visualization of the learned policies. Action output is from -1.0 (red) to 1.0 (blue). Horizontal lines in solid indicate the initial car position distribution $x \sim U(-0.6, -0.4)$, and vertical lines in solid indicate the goal $x > 0.45$. Dashed curves are trajectories starting from the same initial state.

Learning compact policies. The derivative-free nature of ZOAC allows us to estimate the zeroth-order policy gradient to improve the policy without considering the specific policy architecture. Hence, ZOAC can be applied seamlessly to arbitrary parameterized policies in theory, no matter differentiable or not. As a showcase, we further apply ZOAC on two more neural policies with compact structures: Toeplitz

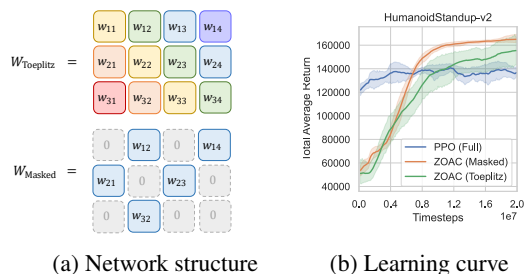


Figure 7: Learning compact policies.

networks that adopt parameter sharing [6] and masked networks that automatically masking out redundant parameters (network architecture search) [18, 41]. Additional detailed introduction of the compact network architecture is attached in Appendix D. We perform additional experiments on two high-dimensional environments. Results in Figure 3a and 7b show that ZOAC successfully trains these compact policies with satisfying performance and much fewer parameters. Non-differentiability is a common reason when turning to evolutionary methods, and ZOAC serves as a more efficient and promising alternative to these methods and therefore has great potential in application.

4.2 Ablation Studies

To evaluate the contribution of each individual component and also the potential of additional techniques, we perform ablation studies and present the results in Figure 8. Results demonstrate that the critic network is a crucial part of ZOAC, i.e., N -step accumulative reward without bootstrapping is not sufficient to guide policy improvement. Observation normalization technique is also essential to zeroth-order methods, which helps to generate diverse policies via isotropic Gaussian noise. Mania et al. [23] propose to use only the top performing directions in policy update to relieve the bad influence of noisy evaluation results and validate its effectiveness on ARS. Here we perform a similar direction sifting technique, using only the directions that have the highest advantage in policy improvement, but it does not seem helpful to the learning performance of ZOAC.

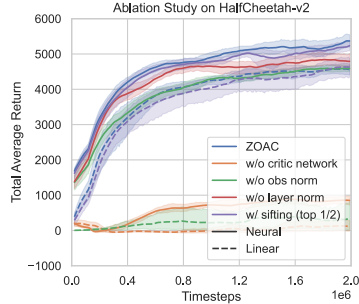


Figure 8: Ablation study

5 Conclusion and Future Work

In this paper, we propose Zeroth-Order Actor-Critic algorithm (ZOAC) that unifies evolution-based zeroth-order and policy gradient-based first-order methods into an on-policy actor-critic architecture to preserve the advantages from both, including the ability to handle different forms of policies, state-dependent exploration, robustness-seeking property from the former and high sample efficiency from the latter. ZOAC conducts rollouts collection with timestep-wise perturbation in parameter space, first-order policy evaluation (PEV) and zeroth-order policy improvement (PIM) alternately in each iteration. Experimental results in a range of challenging continuous control tasks show the superior performance of ZOAC. Ablation studies on hyperparameters and components are also performed to show the properties of ZOAC.

Limitations and Social Impact. The main innovation of our work lies in nicely unifying ES and RL into an on-policy actor-critic architecture and propose a simple yet efficient practical algorithm based on this framework. Although ZOAC has made great progress compared with popular zeroth-order baselines and on-policy first-order baselines, the current version of ZOAC does not reuse any samples for policy improvement and still used traditional isotropic Gaussian noise for perturbation. Advanced techniques from both sides (e.g., sample reuse via importance sampling, constrained update from RL side, and advanced mutation, crossover and elitism technique from ES side) are in theory compatible with our proposed framework and very likely to further improve the performance. Besides, evolution-based methods have been used successfully in various kind of RL problems where common DRL methods are unavailable, like optimizing hierarchical policies [13], searching for symbolic or programmatic policies [20] and so on. Substituting the original evolution-based methods with ZOAC on these tasks may bring encouraging results. We leave the extension of ZOAC and its application on more tasks as our future work.

References

- [1] M. Andrychowicz, A. Raichuk, P. Stańczyk, M. Orsini, S. Girgin, R. Marinier, L. Hussenot, M. Geist, O. Pietquin, M. Michalski, S. Gelly, and O. Bachem. What matters for on-policy deep actor-critic methods? a large-scale study. In *International Conference on Learning Representations*, 2021.

- [2] J. L. Ba, J. R. Kiros, and G. E. Hinton. Layer normalization. *arXiv preprint arXiv:1607.06450*, 2016.
- [3] A. S. Berahas, L. Cao, K. Choromanski, and K. Scheinberg. A theoretical and empirical comparison of gradient approximations in derivative-free optimization. *Foundations of Computational Mathematics*, pages 1–54, 2021.
- [4] C. Bodnar, B. Day, and P. Lió. Proximal distilled evolutionary reinforcement learning. In *Proceedings of the AAAI Conference on Artificial Intelligence*, volume 34, pages 3283–3290, 2020.
- [5] G. Brockman, V. Cheung, L. Pettersson, J. Schneider, J. Schulman, J. Tang, and W. Zaremba. Openai gym. *arXiv preprint arXiv:1606.01540*, 2016.
- [6] K. Choromanski, M. Rowland, V. Sindhvani, R. Turner, and A. Weller. Structured evolution with compact architectures for scalable policy optimization. In *International Conference on Machine Learning*, pages 970–978. PMLR, 2018.
- [7] K. Choromanski, A. Pacchiano, J. Parker-Holder, Y. Tang, and V. Sindhvani. From complexity to simplicity: Adaptive es-active subspaces for blackbox optimization. *Advances in Neural Information Processing Systems*, 32:10299–10309, 2019.
- [8] E. Conti, V. Madhavan, F. P. Such, J. Lehman, K. O. Stanley, and J. Clune. Improving exploration in evolution strategies for deep reinforcement learning via a population of novelty-seeking agents. In *Proceedings of the 32nd International Conference on Neural Information Processing Systems*, pages 5032–5043, 2018.
- [9] M. Fortunato, M. G. Azar, B. Piot, J. Menick, M. Hessel, I. Osband, A. Graves, V. Mnih, R. Munos, D. Hassabis, O. Pietquin, C. Blundell, and S. Legg. Noisy networks for exploration. In *International Conference on Learning Representations*, 2018.
- [10] W. Grathwohl, D. Choi, Y. Wu, G. Roeder, and D. Duvenaud. Backpropagation through the void: Optimizing control variates for black-box gradient estimation. In *International Conference on Learning Representations*, 2018.
- [11] D. Ha and J. Schmidhuber. World models. *arXiv preprint arXiv:1803.10122*, 2018.
- [12] P. Izmailov, D. Podoprikin, T. Garipov, D. Vetrov, and A. G. Wilson. Averaging weights leads to wider optima and better generalization. *arXiv preprint arXiv:1803.05407*, 2018.
- [13] D. Jain, A. Iscen, and K. Caluwaerts. From pixels to legs: Hierarchical learning of quadruped locomotion. *arXiv preprint arXiv:2011.11722*, 2020.
- [14] A. Kendall, J. Hawke, D. Janz, P. Mazur, D. Reda, J.-M. Allen, V.-D. Lam, A. Bewley, and A. Shah. Learning to drive in a day. In *2019 International Conference on Robotics and Automation (ICRA)*, pages 8248–8254. IEEE, 2019.
- [15] N. S. Keskar, D. Mudigere, J. Nocedal, M. Smelyanskiy, and P. T. P. Tang. On large-batch training for deep learning: Generalization gap and sharp minima. *arXiv preprint arXiv:1609.04836*, 2016.
- [16] S. Khadka and K. Tumer. Evolution-guided policy gradient in reinforcement learning. In *Proceedings of the 32nd International Conference on Neural Information Processing Systems*, pages 1196–1208, 2018.
- [17] J. Lehman, J. Chen, J. Clune, and K. O. Stanley. Es is more than just a traditional finite-difference approximator. In *Proceedings of the Genetic and Evolutionary Computation Conference*, pages 450–457, 2018.
- [18] K. Lenc, E. Elsen, T. Schaul, and K. Simonyan. Non-differentiable supervised learning with evolution strategies and hybrid methods. *arXiv preprint arXiv:1906.03139*, 2019.
- [19] E. Liang, R. Liaw, R. Nishihara, P. Moritz, R. Fox, K. Goldberg, J. Gonzalez, M. Jordan, and I. Stoica. Rllib: Abstractions for distributed reinforcement learning. In *International Conference on Machine Learning*, pages 3053–3062. PMLR, 2018.

- [20] A. Likmeta, A. M. Metelli, A. Tirinzoni, R. Giol, M. Restelli, and D. Romano. Combining reinforcement learning with rule-based controllers for transparent and general decision-making in autonomous driving. *Robotics and Autonomous Systems*, 131:103568, 2020.
- [21] T. P. Lillicrap, J. J. Hunt, A. Pritzel, N. Heess, T. Erez, Y. Tassa, D. Silver, and D. Wierstra. Continuous control with deep reinforcement learning. *arXiv preprint arXiv:1509.02971*, 2015.
- [22] N. Maheswaranathan, L. Metz, G. Tucker, D. Choi, and J. Sohl-Dickstein. Guided evolutionary strategies: Augmenting random search with surrogate gradients. In *International Conference on Machine Learning*, pages 4264–4273. PMLR, 2019.
- [23] H. Mania, A. Guy, and B. Recht. Simple random search of static linear policies is competitive for reinforcement learning. In *Proceedings of the 32nd International Conference on Neural Information Processing Systems*, pages 1805–1814, 2018.
- [24] V. Mnih, K. Kavukcuoglu, D. Silver, A. A. Rusu, J. Veness, M. G. Bellemare, A. Graves, M. Riedmiller, A. K. Fidjeland, G. Ostrovski, et al. Human-level control through deep reinforcement learning. *nature*, 518(7540):529–533, 2015.
- [25] V. Mnih, A. P. Badia, M. Mirza, A. Graves, T. Lillicrap, T. Harley, D. Silver, and K. Kavukcuoglu. Asynchronous methods for deep reinforcement learning. In *International conference on machine learning*, pages 1928–1937. PMLR, 2016.
- [26] P. Moritz, R. Nishihara, S. Wang, A. Tumanov, R. Liaw, E. Liang, M. Elibol, Z. Yang, W. Paul, M. I. Jordan, et al. Ray: A distributed framework for emerging {AI} applications. In *13th {USENIX} Symposium on Operating Systems Design and Implementation ({OSDI} 18)*, pages 561–577, 2018.
- [27] Y. Nesterov and V. Spokoiny. Random gradient-free minimization of convex functions. *Foundations of Computational Mathematics*, 17(2):527–566, 2017.
- [28] M. Plappert, R. Houthoofd, P. Dhariwal, S. Sidor, R. Y. Chen, X. Chen, T. Asfour, P. Abbeel, and M. Andrychowicz. Parameter space noise for exploration. In *International Conference on Learning Representations*, 2018.
- [29] A. Pourchot and O. Sigaud. Cem-rl: Combining evolutionary and gradient-based methods for policy search. *arXiv preprint arXiv:1810.01222*, 2018.
- [30] A. Pourchot, N. Perrin, and O. Sigaud. Importance mixing: Improving sample reuse in evolutionary policy search methods. *arXiv preprint arXiv:1808.05832*, 2018.
- [31] H. Qian and Y. Yu. Derivative-free reinforcement learning: A review. *arXiv preprint arXiv:2102.05710*, 2021.
- [32] A. Raffin, A. Hill, M. Ernestus, A. Gleave, A. Kanervisto, and N. Dormann. Stable baselines3. *GitHub repository*, 2019.
- [33] S. Risi and K. O. Stanley. Deep neuroevolution of recurrent and discrete world models. In *Proceedings of the Genetic and Evolutionary Computation Conference*, pages 456–462, 2019.
- [34] T. Salimans, J. Ho, X. Chen, S. Sidor, and I. Sutskever. Evolution strategies as a scalable alternative to reinforcement learning. *arXiv preprint arXiv:1703.03864*, 2017.
- [35] J. Schulman, P. Moritz, S. Levine, M. Jordan, and P. Abbeel. High-dimensional continuous control using generalized advantage estimation. *arXiv preprint arXiv:1506.02438*, 2015.
- [36] J. Schulman, F. Wolski, P. Dhariwal, A. Radford, and O. Klimov. Proximal policy optimization algorithms. *arXiv preprint arXiv:1707.06347*, 2017.
- [37] F. Sehnke, C. Osendorfer, T. Rückstieß, A. Graves, J. Peters, and J. Schmidhuber. Parameter-exploring policy gradients. *Neural Networks*, 23(4):551–559, 2010.
- [38] O. Sener and V. Koltun. Learning to guide random search. In *International Conference on Learning Representations*, 2020.

- [39] O. Sigaud and F. Stulp. Policy search in continuous action domains: an overview. *Neural Networks*, 113:28–40, 2019.
- [40] D. Silver, G. Lever, N. Heess, T. Degris, D. Wierstra, and M. Riedmiller. Deterministic policy gradient algorithms. In *International conference on machine learning*, pages 387–395. PMLR, 2014.
- [41] X. Song, K. Choromanski, J. Parker-Holder, Y. Tang, Q. Zhang, D. Peng, D. Jain, W. Gao, A. Pacchiano, T. Sarlos, and Y. Yang. Es-enas: Blackbox optimization over hybrid spaces via combinatorial and continuous evolution, 2021.
- [42] K. O. Stanley, J. Clune, J. Lehman, and R. Miikkulainen. Designing neural networks through neuroevolution. *Nature Machine Intelligence*, 1(1):24–35, 2019.
- [43] F. P. Such, V. Madhavan, E. Conti, J. Lehman, K. O. Stanley, and J. Clune. Deep neuroevolution: Genetic algorithms are a competitive alternative for training deep neural networks for reinforcement learning. *arXiv preprint arXiv:1712.06567*, 2017.
- [44] R. S. Sutton and A. G. Barto. *Reinforcement learning: An introduction*. MIT press, 2018.
- [45] R. S. Sutton, D. A. McAllester, S. P. Singh, and Y. Mansour. Policy gradient methods for reinforcement learning with function approximation. In *Advances in neural information processing systems*, pages 1057–1063, 2000.
- [46] Y. Tang, K. Choromanski, and A. Kucukelbir. Variance reduction for evolution strategies via structured control variates. In *International Conference on Artificial Intelligence and Statistics*, pages 646–656. PMLR, 2020.
- [47] E. Todorov, T. Erez, and Y. Tassa. Mujoco: A physics engine for model-based control. In *2012 IEEE/RSJ International Conference on Intelligent Robots and Systems*, pages 5026–5033. IEEE, 2012.
- [48] R. J. Williams. Simple statistical gradient-following algorithms for connectionist reinforcement learning. *Machine learning*, 8(3):229–256, 1992.
- [49] T. Zhao, H. Hachiya, G. Niu, and M. Sugiyama. Analysis and improvement of policy gradient estimation. *Advances in Neural Information Processing Systems*, 24:262–270, 2011.

A Related Work

ZOO and its applications in RL. At each iteration, ZOO samples several random directions from a certain distribution, and then the distribution is updated according to the evaluation results over these directions. Sehnke et al. [37] derive parameter-exploring policy gradients (PGPE) for episodic RL problems, which has reduced variance and higher performance than vanilla policy gradient. Salimans et al. [34] and Such et al. [43] propose highly scalable evolution strategies (ES) and genetic algorithms (GA) respectively, both of which can be applied to deep neural networks and achieve competitive performance with MDP-based RL algorithms. Mania et al. [23] propose augmented random search (ARS), which applied ZOO to linear policies with techniques including observation normalization, reward scaling, top performing directions sifting, and achieve astonishing performance on RL benchmarks considering its simplicity. ZOO has regained popularity in recent years because of its special advantages when applied in RL, including wide adaptability to policy parameterization (e.g., deterministic or stochastic, differentiable or non-differentiable), robustness seeking property, state-dependent and temporally-extended exploration.

Improved techniques for ZOO. The main limitation of ZOO is its high sample complexity. Researchers have proposed various improved techniques for ZOO from different perspectives. One way is to adopt advanced Monte Carlo sampling methods to reduce variance of the zeroth-order gradient estimation, e.g., antithetic sampling [37, 34, 23], orthogonal and Quasi Monte Carlo exploration [6]. Constructing control variates (i.e., subtracting a baseline) is another popular variance reduction technique. Sehnke et al. [37] adopt a moving-average baseline in PGPE heuristically, while Zhao et al. [49] derive the optimal baseline for PGPE in an analytical form that minimizes the variance. Moreover, the sample complexity of zeroth-order methods will further increase with the dimension of the optimization problem [27], therefore some researches aim to identify a low-dimensional search space and guide the search towards faster convergence. Guided ES [22] and ASEBO [7] are proposed based on a similar idea: to identify linear subspaces and adapt the search distribution from recent history of descent directions. Sener and Koltun [38] propose LMRS, which jointly learns the underlying subspace represented by neural networks and optimizes the objective function.

Hybridization of ZOO and first-order MDP-based RL. These two methods have complementary advantages when applied to RL problems, and recent researches have tried to combine them for better performance. Khadka and Tumer [16] propose the ERL framework that runs evolutionary algorithms (EA) and DDPG [21] concurrently with bidirectional information flow, i.e., the DDPG agent is trained with experiences generated by the EA population and reinserted into the population periodically to guide the evolution process. CEM-RL [29] and Proximal Distilled ERL [4] adopt similar hybridization framework, but use different algorithms as components and improve training techniques. Fortunato et al. [9] and Plappert et al. [28] inject parameter noises into existing first-order MDP-based RL algorithms to drive more efficient exploration, and demonstrate that existing RL algorithms can indeed benefit from parameter space exploration through comparative experiments. Some other hybrid methods [10, 46] leverage policy gradient and reparameterization trick to construct control variates, which leads to unbiased, low variance gradient estimators. Our proposed method, however, unifies first-order and zeroth-order methods into an on-policy actor-critic architecture by conducting first-order PEV and zeroth-order PIM alternately in each iteration. The state-value function network does not only serve as a baseline to reduce variance, but also as a critic used for bootstrapping, which leads to reduced variance and accelerated learning [44]. The policy is updated in a zeroth-order way, which implies wide adaptability to different forms of policies.

B Proofs

B.1 Proof of Theorem 1

Regularity conditions 1: $p(s'|s, a)$, $\pi_\theta(s)$, $r(s, a)$, $d_0(s)$ are continuous in all parameters and variables s , a , s' .

Theorem 1. For MDP that satisfies regularity conditions 1, zeroth-order policy gradient of Equation (6) can be presented as:

$$\nabla_{\theta} J_{\text{ZOAC}}(\theta) = \frac{1}{\sigma} \mathbb{E}_{s_t \sim d_{\beta}} \mathbb{E}_{\epsilon \sim \mathcal{N}(0, I)} [Q^{\beta}(s_t, \pi_{\theta + \sigma \epsilon}(s_t)) \epsilon]$$

The following proof follows the policy gradient theorem proved by Sutton et al. [45] and the deterministic policy gradient theorem proved by Silver et al. [40]. The above regularity conditions, together with Leibniz integral rule and Fubini's theorem, enable us to exchange derivatives and integrals, and the order of integration whenever necessary and we do not repeat during the proof.

Proof.

$$\begin{aligned} \nabla_{\theta} V^{\beta}(s) &= \nabla_{\theta} \mathbb{E}_{\epsilon_1 \sim \mathcal{N}(0, I)} [Q^{\beta}(s, \pi_{\theta + \sigma \epsilon_1}(s))] \\ &= \nabla_{\theta} \mathbb{E}_{\epsilon_1 \sim \mathcal{N}(0, I)} \left[r(s, \pi_{\theta + \sigma \epsilon_1}(s)) + \int_{\mathcal{S}} \gamma p(s' | s, \pi_{\theta + \sigma \epsilon_1}(s)) V^{\beta}(s') ds' \right] \\ &= \frac{1}{\sigma} \mathbb{E}_{\epsilon_1 \sim \mathcal{N}(0, I)} \left[\left(r(s, \pi_{\theta + \sigma \epsilon_1}(s)) + \int_{\mathcal{S}} \gamma p(s' | s, \pi_{\theta + \sigma \epsilon_1}(s)) V^{\beta}(s') ds' \right) \epsilon_1 \right] \\ &\quad + \mathbb{E}_{\epsilon_1 \sim \mathcal{N}(0, I)} \int_{\mathcal{S}} \gamma p(s' | s, \pi_{\theta + \sigma \epsilon_1}(s)) \nabla_{\theta} V^{\beta}(s') ds' \\ &= \frac{1}{\sigma} \mathbb{E}_{\epsilon_1 \sim \mathcal{N}(0, I)} [Q^{\beta}(s, \pi_{\theta + \sigma \epsilon_1}(s)) \epsilon_1] \\ &\quad + \mathbb{E}_{\epsilon_1 \sim \mathcal{N}(0, I)} \int_{\mathcal{S}} \gamma p(s \rightarrow s', 1, \pi_{\theta + \sigma \epsilon_1}) \nabla_{\theta} V^{\beta}(s') ds' \end{aligned}$$

Note that in the above derivation, we use the zeroth-order gradient trick as in Equation (4) in some of the terms, i.e.:

$$\nabla_{\theta} \mathbb{E}_{\epsilon \sim \mathcal{N}(0, I)} f(\theta + \sigma \epsilon) = \frac{1}{\sigma} \mathbb{E}_{\epsilon \sim \mathcal{N}(0, I)} [f(\theta + \sigma \epsilon) \epsilon]$$

We continue to unroll the recursive representation of $\nabla_{\theta} V^{\beta}(s)$:

$$\begin{aligned} \nabla_{\theta} V^{\beta}(s) &= \frac{1}{\sigma} \mathbb{E}_{\epsilon_1 \sim \mathcal{N}(0, I)} [Q^{\beta}(s, \pi_{\theta + \sigma \epsilon_1}(s)) \epsilon_1] \\ &\quad + \frac{1}{\sigma} \mathbb{E}_{\epsilon_1 \sim \mathcal{N}(0, I)} \int_{\mathcal{S}} \gamma p(s \rightarrow s', 1, \pi_{\theta + \sigma \epsilon_1}) \mathbb{E}_{\epsilon_2 \sim \mathcal{N}(0, I)} [Q^{\beta}(s', \pi_{\theta + \sigma \epsilon_2}(s')) \epsilon_2] ds' \\ &\quad + \mathbb{E}_{\epsilon_1 \sim \mathcal{N}(0, I)} \int_{\mathcal{S}} \gamma p(s \rightarrow s', 1, \pi_{\theta + \sigma \epsilon_1}) \mathbb{E}_{\epsilon_2 \sim \mathcal{N}(0, I)} \int_{\mathcal{S}} \gamma p(s' \rightarrow s'', 1, \pi_{\theta + \sigma \epsilon_2}) \nabla_{\theta} V^{\beta}(s'') ds'' ds' \end{aligned}$$

Since the behavior policy β is exactly the stochastic version of π_{θ} with Gaussian parameter noise ϵ sampled i.i.d. at every timesteps, we can rewrite and continue to iterate the above formula:

$$\begin{aligned} \nabla_{\theta} V^{\beta}(s) &= \frac{1}{\sigma} \mathbb{E}_{\epsilon \sim \mathcal{N}(0, I)} [Q^{\beta}(s, \pi_{\theta + \sigma \epsilon}(s)) \epsilon] \\ &\quad + \int_{\mathcal{S}} \gamma p(s \rightarrow s', 1, \beta) \frac{1}{\sigma} \mathbb{E}_{\epsilon \sim \mathcal{N}(0, I)} [Q^{\beta}(s', \pi_{\theta + \sigma \epsilon}(s')) \epsilon] ds' \\ &\quad + \int_{\mathcal{S}} \gamma^2 p(s \rightarrow s', 2, \beta) \nabla_{\theta} V^{\beta}(s') ds' \\ &= \dots \\ &= \int_{\mathcal{S}} \sum_{t=0}^{\infty} \gamma^t p(s \rightarrow s', t, \beta) \frac{1}{\sigma} \mathbb{E}_{\epsilon \sim \mathcal{N}(0, I)} [Q^{\beta}(s', \pi_{\theta + \sigma \epsilon}(s')) \epsilon] ds' \end{aligned}$$

Now we can derive the zeroth-order policy gradient by taking the expectation over initial state distribution:

$$\begin{aligned}
\nabla_{\theta} J_{\text{ZOAC}}(\theta) &= \nabla_{\theta} \mathbb{E}_{s \sim d_0} [V^{\beta}(s)] \\
&= \int_{\mathcal{S}} d_0(s) \nabla_{\theta} V^{\beta}(s) ds \\
&= \int_{\mathcal{S}} \int_{\mathcal{S}} \sum_{t=0}^{\infty} \gamma^t d_0(s) p(s \rightarrow s', t, \beta) \frac{1}{\sigma} \mathbb{E}_{\epsilon \sim \mathcal{N}(0, I)} [Q^{\beta}(s', \pi_{\theta+\sigma\epsilon}(s')) \epsilon] ds' ds \\
&= \frac{1}{\sigma} \int_{\mathcal{S}} d_{\beta}(s) \mathbb{E}_{\epsilon \sim \mathcal{N}(0, I)} [Q^{\beta}(s, \pi_{\theta+\sigma\epsilon}(s)) \epsilon] ds \\
&= \frac{1}{\sigma} \mathbb{E}_{s \sim d_{\beta}} \mathbb{E}_{\epsilon \sim \mathcal{N}(0, I)} [Q^{\beta}(s, \pi_{\theta+\sigma\epsilon}(s)) \epsilon]
\end{aligned}$$

□

B.2 Proof of Theorem 2

Theorem 2. *If the reward $|r(s, a)| < \alpha$, the critic network output $|V_w(s)| < \varphi$, and n trajectories with length of $N \times H$ timesteps are collected in one iteration, the upper bounds of the variance of gradient estimators in Eq. (10) and (11) are:*

$$\begin{aligned}
\text{Var}[\nabla_{\theta} \hat{J}_{\text{ES}}(\theta)] &\leq \frac{(1 - \gamma^{NH})^2 \alpha^2 d}{n\sigma^2(1 - \gamma)^2} \\
\text{Var}[\nabla_{\theta} \hat{J}_{\text{ZOAC}}(\theta)] &\leq \frac{((1 - \gamma^N)\alpha + (1 - \gamma)(1 + \gamma^N)\varphi)^2 d}{nH\sigma^2(1 - \gamma)^2}
\end{aligned}$$

The following proof follows the variance analysis scheme provided in [49].

Proof. (1) Variance bound for ES gradient estimators

Under the setting described in Section 3.2, the state-value under policy $\pi_{\theta+\sigma\epsilon}$ is estimated by the accumulative return over NH timesteps, which is denoted as $\hat{V}_{NH}^{\pi_{\theta+\sigma\epsilon}}$. The isotropic Gaussian noise added to the policy can be presented as $\epsilon = (\epsilon_1, \epsilon_2, \dots, \epsilon_d)^{\top}$, where $\epsilon_l \sim \mathcal{N}(0, 1)$, $l \in \{1, 2, \dots, d\}$.

$$\begin{aligned}
\text{Var}[\hat{V}_{NH}^{\pi_{\theta+\sigma\epsilon}} \epsilon] &\leq \sum_{l=1}^d \mathbb{E}[(\hat{V}_{NH}^{\pi_{\theta+\sigma\epsilon}} \epsilon_l)^2] \\
&= \sum_{l=1}^d \int p(\epsilon_l) \left(\sum_{t=1}^{NH} \gamma^{t-1} r(s_t, a_t) \right)^2 \epsilon_l^2 d\epsilon_l \\
&\leq \sum_{l=1}^d \int p(\epsilon_l) \left(\sum_{t=1}^{NH} \gamma^{t-1} \alpha \right)^2 \epsilon_l^2 d\epsilon_l \\
&= \frac{(1 - \gamma^{NH})^2 \alpha^2}{(1 - \gamma)^2} \sum_{l=1}^d \int p(\epsilon_l) \epsilon_l^2 d\epsilon_l \\
&= \frac{(1 - \gamma^{NH})^2 \alpha^2}{(1 - \gamma)^2} \sum_{l=1}^d \mathbb{E}_{\epsilon_l \sim \mathcal{N}(0, 1)} \epsilon_l^2 \\
&= \frac{(1 - \gamma^{NH})^2 \alpha^2 d}{(1 - \gamma)^2}
\end{aligned}$$

The last equality holds because $\epsilon_l^2 \sim \chi^2(1)$ when $\epsilon_l \sim \mathcal{N}(0, 1)$, and $\mathbb{E}[\epsilon_l^2] = 1$ for all l . Since n random directions are sampled and evaluated, the ES gradient estimator is given according to Equation (10):

$$\nabla_{\theta} \hat{J}_{\text{ES}}(\theta) = \frac{1}{n\sigma} \sum_{i=1}^n \hat{V}_{NH}^{\pi_{\theta+\sigma\epsilon_i}} \epsilon_i$$

Therefore the variance bound for ES can be derived as:

$$\begin{aligned}\text{Var}[\nabla_{\theta} \hat{J}_{\text{ES}}(\theta)] &= \frac{1}{n\sigma^2} \text{Var}[\hat{V}_{NH}^{\pi_{\theta+\sigma\epsilon}} \epsilon] \\ &\leq \frac{(1-\gamma^{NH})^2 \alpha^2 d}{n\sigma^2(1-\gamma)^2}\end{aligned}$$

(2) Variance bound for ZOAC gradient estimators

As stated in Section 3.2, the fitness score of policy $\pi_{\theta+\sigma\epsilon}$ is estimated by the N -step TD residual, which is denoted as $\hat{A}_N^{\pi_{\theta+\sigma\epsilon}}$. The isotropic Gaussian noise ϵ is added to the policy as well.

$$\begin{aligned}\text{Var}[\hat{A}_N^{\pi_{\theta+\sigma\epsilon}} \epsilon] &\leq \sum_{l=1}^d \mathbb{E}[(\hat{A}_N^{\pi_{\theta+\sigma\epsilon}} \epsilon_l)^2] \\ &= \sum_{l=1}^d \int p(\epsilon_l) \left(\sum_{t=1}^N \gamma^{t-1} r(s_t, a_t) + \gamma^N V_w(s_{t+N}) - V_w(s_t) \right)^2 \epsilon_l^2 d\epsilon_l \\ &\leq \sum_{l=1}^d \int p(\epsilon_l) \left(\sum_{t=1}^N \gamma^{t-1} \alpha + (1+\gamma^N)\varphi \right)^2 \epsilon_l^2 d\epsilon_l \\ &= \left(\frac{(1-\gamma^N)\alpha + (1-\gamma)(1+\gamma^N)\varphi}{(1-\gamma)} \right)^2 \sum_{l=1}^d \int p(\epsilon_l) \epsilon_l^2 d\epsilon_l \\ &= \left(\frac{(1-\gamma^N)\alpha + (1-\gamma)(1+\gamma^N)\varphi}{(1-\gamma)} \right)^2 d\end{aligned}$$

Totally $n \times H$ random directions is sampled and evaluated, and the ZOAC gradient estimator is given according to Equation (11):

$$\nabla_{\theta} \hat{J}_{\text{ZOAC}}(\theta) \approx \frac{1}{nH\sigma} \sum_{i=1}^{nH} \hat{A}_N^{\pi_{\theta+\sigma\epsilon_i}} \epsilon_i$$

Therefore the variance bound for ZOAC can be derived:

$$\begin{aligned}\text{Var}[\nabla_{\theta} \hat{J}_{\text{ZOAC}}(\theta)] &= \frac{1}{nH\sigma^2} \text{Var}[\hat{A}_N^{\pi_{\theta+\sigma\epsilon}} \epsilon] \\ &\leq \frac{((1-\gamma^N)\alpha + (1-\gamma)(1+\gamma^N)\varphi)^2 d}{nH\sigma^2(1-\gamma)^2}\end{aligned}$$

□

C Implementation Details

We implemented ZOAC with parallelized workers (Algorithm 1) using the distributed framework Ray [26]. We follow the parallelization techniques used in ES [34] and ARS [23]. Firstly, we created a shared noise table before training starts, then the workers communicate indices in the shared table but not the perturbation vectors, so as to avoid high communication cost. Besides, random seeds for constructing parallelized training environments and the evaluation environment are different and generated from a single seed designated before hand.

We use two different types of policies: linear policies for ARS and ZOAC (linear), neural networks with (64, 64) hidden nodes and tanh nonlinearities for ES, PPO and ZOAC (neural). For actor-critic algorithms, we use neural networks with (256, 256) hidden nodes and tanh nonlinearities as critics to estimate state-value function.

Both the zeroth-order baseline methods perform reward shaping to resolve the local optima problem as described in the original paper: ARS subtracts the survival bonus from rewards (1 in Hopper-v2

and Ant-v2), while ES transforms the episodic returns into rankings. ES further discretize the actions to encourage exploration in Hopper-v2 but we do not reserve this trick for comparison since discretization will lead to a different policy architecture. ZOAC, however, does not rely on domain-specific heuristic tricks, which can be attributed to the construction of advantage estimators in policy improvement.

We summarize the hyperparameters used in ZOAC in Table 1 and list their values that are used to produce the results in Figure 4. During evaluation, exploration noise are turned off and the reported total average return is averaged over 10 episodes.

Table 1: Hyperparameters of ZOAC for the learning curves shown in Figure 4

Environment	InvertedDP		Hopper		HalfCheetah		Ant		HStand	
	L	N	L	N	L	N	L	N	L	N
Policy type	L	N	L	N	L	N	L	N	L	N
Num. of workers n	8									
Rollout length N	10									
Train frequency H	16						128			
Para. noise std. σ	0.03		0.05		0.06		0.03			
Batch size L	64						128			
Num. of epochs M	8						4			
Actor optimizer	Adam($\alpha_{\text{actor}} = 0.005, \beta_1 = 0.9, \beta_2 = 0.999$)						$\alpha_{\text{actor}} = 0.003$			
Critic optimizer	Adam($\alpha_{\text{critic}} = 0.0003, \beta_1 = 0.9, \beta_2 = 0.999$)									
Discount factor γ	0.99						0.99			
GAE coeff. λ	0.95						0.95			

D Details of the Compact Policies

Fully connected neural network can be presented as the connection of the following function in series:

$$y = f(W, b) = \phi(Wx + b) \tag{18}$$

where $x \in \mathbb{R}^n$ refers to the input vector, $y \in \mathbb{R}^m$ refers to the output vector, $W \in \mathbb{R}^{m \times n}$ refers to weight parameters, $b \in \mathbb{R}^m$ refers to bias parameters, and ϕ refers to element-wise nonlinear activation function.

Here we consider two different types of compact neural networks that compress the weight matrix W at each layer, to achieve a parameter number less than $m \times n$.

The first one is called Toeplitz network from [6]. Toeplitz matrix is a kind of compact matrix with parameter sharing schemes, each element depends only on the difference between the row index and the column index. Hence, a Toeplitz matrix $T \in \mathbb{R}^{m \times n}$ has only $m + n - 1$ parameters.

The second one is called masked network from [18, 41]. It reduces the number of independent parameters by masking out redundant parameters (i.e., pruning). It setups another mask weight matrix $M \in \mathbb{R}^{m \times n}$. The near binary mask is then generated via $M' = \text{softmax}(M/\alpha)$. Softmax operation is applied element-wise and α is chosen to be 0.01. All parameters are concatenated and optimized using ZOAC. In order to encourage less parameters, we modify the advantage of each perturbed directions to be $A' = \beta A + (1 - \beta)(1 - \lambda)$, where A is the original normalized advantage function, λ is the usage of weight matrix parameters (i.e. effective edges), and $\beta \in [0, 1]$ is a weighting factor that anneals as training progresses.

Table 2 compares the dimension of different networks, in which the dimension of masked networks presents the average value after convergence over 10 trails. Figure 9 shows an instance of sparse policy learned by ZOAC in Ant-v2 environments that achieves around 4500 cumulative return with only about 10% of all available connections.

